CrossMark click for updates

Epigenetic inactivation of the p53-induced long noncoding RNA TP53 target 1 in human cancer

Angel Diaz-Lagares[a], Ana B. Crujeiras[a,b,c], Paula Lopez-Serra[a], Marta Soler[a], Fernando Setien[a], Ashish Goyal[d,e], Juan Sandoval[a], Yutaka Hashimoto[a], Anna Martinez-Cardús[a], Antonio Gomez[a], Holger Heyn[a], Catia Moutinho[a], Jesús Espada[f,g], August Vidal[h], Maria Paúles[h], Maica Galán[i], Núria Sala[j], Yoshimitsu Akiyama[k], María Martínez-Iniesta[l], Lourdes Farré[l,m], Alberto Villanueva[l], Matthias Gross[d,e], Sven Diederichs[d,e,n,o,p], Sonia Guil[a,1], and Manel Esteller[a,q,r,1]

[a]Cancer Epigenetics and Biology Program (PEBC), Bellvitge Biomedical Research Institute (IDIBELL), L'Hospitalet de Llobregat, 08908 Barcelona, Catalonia, Spain; [b]Centro de Investigación Biomédica en Red (CIBER) Fisiopatología de la Obesidad y Nutrición (CIBERobn), Instituto Salud Carlos III, 28029 Madrid, Spain; [c]Endocrine Division, Complejo Hospitalario Universitario de Santiago, 15706 Santiago de Compostela, Spain; [d]Division of RNA Biology and Cancer (B150), German Cancer Research Center (DKFZ), 69120 Heidelberg, Germany; [e]Institute of Pathology, University Hospital Heidelberg, 69120 Heidelberg, Germany; [f]Experimental Dermatology and Skin Biology Group, Ramón y Cajal Institute for Biomedical Research (IRYCIS), Ramón y Cajal University Hospital, 28034 Madrid, Spain; [g]Bionanotechnology Laboratory, Bernardo O'Higgins University, Santiago 8370854, Chile; [h]Pathology Department, Hospital Universitari de Bellvitge, IDIBELL, L'Hospitalet de Llobregat, 08907 Barcelona, Catalonia, Spain; [i]Department of Medical Oncology, Catalan Institute of Oncology (ICO), IDIBELL, L'Hospitalet de Llobregat, 08908 Barcelona, Catalonia, Spain; [j]Unit of Nutrition and Cancer, Cancer Epidemiology Research Program, ICO, IDIBELL, 08908 Barcelona, Catalonia, Spain; [k]Department of Molecular Oncology, Graduate School of Medical and Dental Sciences, Tokyo Medical and Dental University, 113-8510 Tokyo, Japan; [l]Program Against Cancer Therapeutic Resistance (ProCURE), ICO, IDIBELL, L'Hospitalet del Llobregat, 08908 Barcelona, Catalonia, Spain; [m]Laboratory of Experimental Pathology (LAPEX), Gonçalo Moniz Research Center, Oswaldo Cruz Foundation (CPQGM/FIOCRUZ) and National Institute of Science and Technology of Tropical Diseases (INCT/DT), 40296710 Salvador, Bahia, Brazil; [n]Division of Cancer Research, Department of Thoracic Surgery, Medical Center–University of Freiburg, 79106 Freiburg, Germany; [o]Faculty of Medicine, University of Freiburg, 79106 Freiburg, Germany; [p]German Cancer Consortium (DKTK), 79106 Freiburg, Germany; [q]Departament de Ciències Fisiològiques II, Escola de Medicina, Universitat de Barcelona, 08907 Barcelona, Catalonia, Spain; and [r]Institució Catalana de Recerca i Estudis Avançats (ICREA), 08010 Barcelona, Catalonia, Spain

Edited by Mariano Barbacid, Spanish National Cancer Research Center (CNIO), Madrid, Spain, and approved October 12, 2016 (received for review May 27, 2016)

Long noncoding RNAs (lncRNAs) are important regulators of cellular homeostasis. However, their contribution to the cancer phenotype still needs to be established. Herein, we have identified a p53-induced lncRNA, TP53TG1, that undergoes cancer-specific promoter hypermethylation-associated silencing. In vitro and in vivo assays identify a tumor-suppressor activity for TP53TG1 and a role in the p53 response to DNA damage. Importantly, we show that TP53TG1 binds to the multifaceted DNA/RNA binding protein YBX1 to prevent its nuclear localization and thus the YBX1-mediated activation of oncogenes. TP53TG1 epigenetic inactivation in cancer cells releases the transcriptional repression of YBX1-targeted growth-promoting genes and creates a chemoresistant tumor. TP53TG1 hypermethylation in primary tumors is shown to be associated with poor outcome. The epigenetic loss of TP53TG1 therefore represents an altered event in an lncRNA that is linked to classical tumoral pathways, such as p53 signaling, but is also connected to regulatory networks of the cancer cell.

DNA methylation | long noncoding RNA | epigenetics | cancer

It has been estimated that only 2% of the genome is transcribed into protein-coding RNAs (1), so most of the transcriptome corresponds to noncoding transcripts, which are classified according to their length and structural properties (2, 3). Among the small noncoding RNAs (ncRNAs), the abundant class of miRNAs (19–25 nt) regulates gene expression through interactions based on their complementarity with target mRNAs (4). These ncRNAs have been widely studied in the context of cancer cells (5, 6). The other main group of ncRNAs is the long ncRNAs (lncRNAs; arbitrarily >200 nt), which are defined as lacking protein-coding potential but otherwise often display mRNA-like properties, including multiexonic gene structures and poly(A) tails (2, 3). LncRNAs are associated with a variety of regulatory functions, including chromatin-related roles, splicing control, and transcriptional regulation (7–9). Despite recent reports describing aberrant expression of lncRNAs in human tumors (8–11), few of these molecules have been carefully characterized with respect to their functional roles in the promotion or inhibition of carcinogenesis (12, 13). However, significant exceptions exist, and mechanisms of action and downstream cellular effects have been demonstrated for lncRNAs acting as oncogenes, such as HOTAIR (14) and MALAT1 (15), or as tumor suppressors, such as LincRNA-p21 (16) and Uc.283+A (17).

Several recent studies have demonstrated that lncRNAs are deregulated in cancer tissues. Causes of this deregulation include genetic events leading to abnormal expression, such as copy number alterations or single-nucleotide polymorphisms located in lncRNA promoter regions (8–11). However, another possibility is that lncRNAs may themselves be targets of epigenetic disruption. In this regard, the promoter CpG island hypermethylation-associated silencing of coding tumor-suppressor genes and microRNAs is a well-established hallmark of human cancer (18–21). In recent times, a relatively small number of lncRNAs, such as

Significance

Long noncoding RNAs (lncRNAs) are starting to be recognized as critical molecules for cellular transformation, although only a few candidates have so far been characterized. Here we report that TP53TG1 is an lncRNA that is critical for the correct response of p53 to DNA damage. The cancer growth suppressor features of TP53TG1 are linked to its ability to block the tumorigenic activity of the RNA binding protein YBX1. The DNA methylation-associated silencing of TP53TG1 produces aggressive tumors that are resistant to cellular death when DNA-damaging agents and small targeted molecules are used. Our study provides an example of a tumor suppressor lncRNA undergoing an epigenetic lesion in cancer that is placed at the crossroads of DNA damage and oncogenic pathways.

Author contributions: A.D.-L., S.G., and M.E. designed research; A.D.-L., A.B.C., P.L.-S., M.S., F.S., A. Goyal, J.S., Y.H., A.M.-C., A. Gomez, H.H., C.M., J.E., A. Vidal, M.P., M. Galan, N.S., Y.A., M.M.-I., L.F., A. Villanueva, M. Gross, S.D., and S.G. performed research; A.D.-L., A.B.C., P.L.-S., M.S., F.S., A. Goyal, J.S., Y.H., A.M.-C., A. Gomez, H.H., C.M., J.E., A. Vidal, M.P., M. Galan, N.S., Y.A., M.M.-I., L.F., A. Villanueva, M. Gross, S.D., S.G., and M.E. analyzed data; and A.D.-L., S.G., and M.E. wrote the paper.

The authors declare no conflict of interest.

This article is a PNAS Direct Submission.

Freely available online through the PNAS open access option.

[1]To whom correspondence may be addressed. Email: mesteller@idibell.cat or sguil@idibell.cat.

This article contains supporting information online at www.pnas.org/lookup/suppl/doi:10.1073/pnas.1608585113/-/DCSupplemental.

transcribed–ultraconserved regions (22), antisense RNAs (23), and small nucleolar RNAs (24), have been shown to undergo cancer-specific epigenetic inactivation, but the field of DNA methylation-dependent silencing of lncRNAs remains largely unexplored. In this study, we have found that the epigenetic loss of the lncRNA TP53TG1 enhances tumor progression, prevents an effective p53 response to DNA damage, creates a chemoresistant phenotype, and unleashes the transforming capacities of its partner, identified herein, the RNA binding protein YBX1.

Results

TP53TG1 Shows Cancer-Specific DNA Methylation-Associated Transcriptional Silencing. To characterize cancer-specific DNA methylation changes that affect lncRNA expression, we followed the experimental workflow shown in Fig. 1*A*. We took advantage of the existence of an isogenic cell line derived from the colon cancer cell line HCT-116, which shows genetic disruption by homologous recombination of the DNA methyltransferase 1 (DNMT1) and DNMT3b (double knockout, DKO) (25). DKO cells have drastically reduced DNMT activity, 5-methylcytosine DNA content, and, above all, a release of coding genes and microRNA silencing associated with promoter CpG island hypomethylation (25). We wanted to identify cancer-specific DNA methylation events in lncRNA loci, so we also included two samples of normal colon mucosa in our study design. We obtained the DNA methylation profile of the wild-type HCT-116 cells, the derived DKO cells, and the aforementioned normal colon using the Infinium HumanMethylation450 (450K) microarray, which interrogates 482,422 CpG sites (26). Noting that the platform includes 104 annotated lncRNAs with a 5′-CpG island (*SI Appendix*, Table S1) enabled us to narrow our search to the candidate methylated positions with a possible effect on lncRNA expression. To identify from among these candidates those lncRNAs with cancer-specific differential methylation, we imposed stringent criteria to consider only those CpG island sites with a ≥70% change in the CpG methylation level between the cancer cell

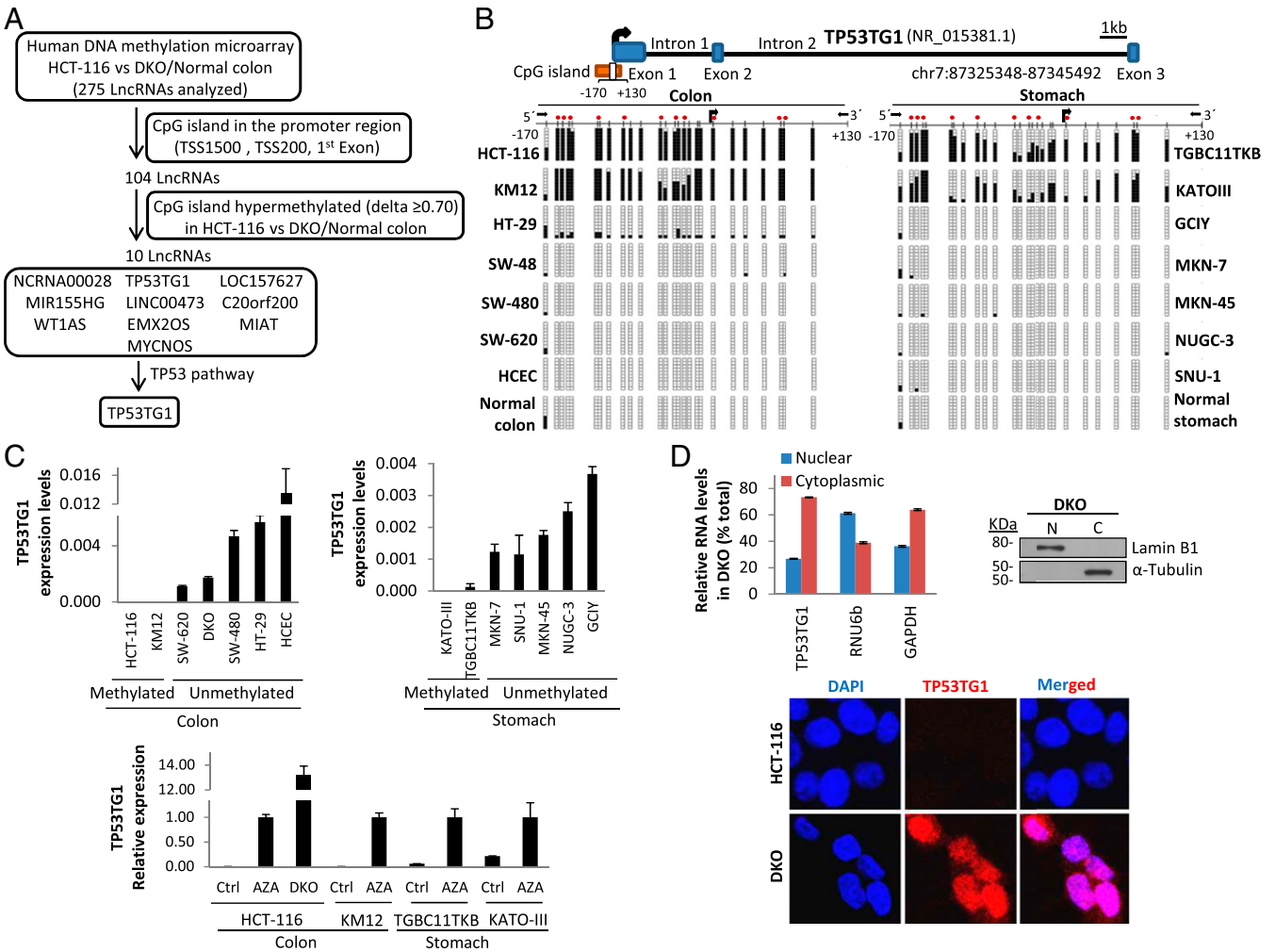

Fig. 1. Epigenetic silencing of the lncRNA TP53TG1 in cancer cells. (*A*) Schematic strategy used to identify tumor-specific DNA methylation events in lncRNAs. (*B*) Bisulfite genomic sequencing analysis of TP53TG1 promoter CpG island in cancer cell lines and normal tissues. Locations of bisulfite genomic sequencing PCR primers (black arrows), CpG dinucleotides (vertical lines), and the TSS (long black arrow) are shown. Ten single clones are represented for each sample. The presence of unmethylated and methylated CpGs is indicated by white and black squares, respectively. Red circles indicate the CpGs detected by the DNA methylation 450K microarray. (*C*) DNA methylation-associated transcriptional silencing of TP53TG1 in cancer cells. (*Upper*) TP53TG1 expression levels in methylated (HCT-116, KM12, and KATOIII) and unmethylated (SW480, HT29, MKN-7, SNU-1, MKN-45, NUGC-3, and GCIY) cancer cell lines determined by qRT-PCR. (*Lower*) Restored TP53TG1 expression after treatment with the DNA demethylating agent 5-aza-2′-deoxycytidine (AZA) or upon genetic depletion (DKO) in the originally methylated cell lines. Values were determined from triplicates and are expressed as the mean ± SEM. (*D*) TP53TG1 RNA-FISH and intracellular localization. (*Upper*) TP53TG1 subcellular distribution in DKO by qRT-PCR. RNAU6b and GAPDH genes were used as controls for the nuclear and cytoplasmic fractions, respectively. Values were determined from triplicates and are expressed as the mean ± SEM. The effectiveness of cell fractionation was evaluated with lamin B1 (nuclear) and tubulin (cytoplasmic) by Western blot. C, cytoplasm; N, nucleus. (*Lower*) Single-molecule visualization of TP53TG1 (red spots) in HCT-116 and DKO cell lines by FISH.

line HCT-116 compared with the demethylated DKO cell line and the normal colon cell line. Under these conditions, we identified 10 targets: TP53TG1 (TP53 target gene 1), NCRNA00028, LOC157627, MIR155HG, WT1AS, LINC00473, C20orf200, EMX2OS, MIAT, and MYCNOS (Fig. 1*A* and *SI Appendix*, Table S2). Quantitative RT-PCR analyses confirmed transcriptional silencing in HCT-116 cells and demethylation-associated reactivation in DKO cells for seven (70%) of the lncRNAs: TP53TG1, NCRNA00028, LOC157627, MIR155HG, WT1AS, C20orf200, and MYCNOS (*SI Appendix*, Fig. S1). Although all of them were promising candidates for further analysis, we decided to focus our interest on TP53TG1 because of its high-ranking order in the differential methylation (*SI Appendix*, Table S2) and expression (*SI Appendix*, Fig. S1) data and because of its proposed role in central cancer pathways such as the p53 network (27). With respect to the latter, TP53TG1 expression is induced in a p53-dependent manner upon conditions of cellular stress that involve the induction of double-strand breaks, such as UV irradiation (27, 28), or exposure to bleomycin or cisplatin (28).

To further demonstrate the silencing of TP53TG1 in cancer cells in association with the presence of promoter CpG island hypermethylation, we proceeded to characterize its transcription start site (TSS) and DNA methylation patterns. Using rapid amplification of cDNA ends (RACE), we confirmed that the TP53TG1 transcript originates within the CpG island in the DNA methylation microarray, confirming the Refseq database annotation in UCSC (NR_015381.1 from GRCh38/hg38). Bisulfite genomic sequencing of multiple clones confirmed the dense methylation of the CpG island in HCT-116 cells and its unmethylated status in normal colorectal mucosa (Fig. 1*B*). We extended our DNA methylation analyses to another 12 gastrointestinal cancer cell lines (Fig. 1*B*). In addition to HCT-116, TP53TG1 5′-end CpG island hypermethylation was also found in the colorectal cancer cell line KM12 and in the gastric cancer cell lines KATO-III and TGBC11TKB. All of the other cell lines were unmethylated at this locus (Fig. 1*B*). Normal gastric mucosa and nontumorigenic human colon epithelial cells (HCECs) (29) were unmethylated at the TP53TG1 CpG island (Fig. 1*B*). Quantitative RT-PCR revealed a loss of TP53TG1 expression in all of the hypermethylated cells, whereas lncRNA was expressed in the unmethylated cases (Fig. 1*C*). Importantly, the use of the demethylating agent 5-aza-2'-deoxycytidine restored TP53TG1 expression in the hypermethylated HCT-116, KM12, KATO-III, and TGBC11TKB cell lines (Fig. 1*C*). Subcellular fractioning showed that the TP53TG1 transcript in DKO cells, in addition to being present in both the cytoplasm and the nucleus, was particularly enriched in the cytosolic compartment (Fig. 1*D*). RNA fluorescence in situ hybridization (RNA-FISH) corroborated this intracellular localization (Fig. 1*D*). We confirmed the noncoding nature of the TP53TG1 RNA transcript by using an artificially created recombinant protein followed by Western blot to demonstrate the lack of any TP53TG1-derived protein in the unmethylated HCEC and DKO cell lines (*SI Appendix*, Fig. S2). In vitro transcription/translation assays confirmed the absence of TP53TG1 coding potential (*SI Appendix*, Fig. S2). TP53TG1's lack of coding capacity was also apparent from the negative codon substitution frequency (CSF) score (30) of –402.4488, which was similar to that obtained from the well-characterized lncRNA HOTAIR (–354.5062). Overall, these results indicate that tumor-specific promoter CpG island hypermethylation-associated silencing of the lncRNA TP53TG1 occurs in colorectal and gastric cancer cells.

TP53TG1 Exhibits Tumor Suppressor-Like Features in Cancer Cells. Having observed the CpG island hypermethylation-associated silencing of TP53TG1 in colorectal and gastric cancer cells, we used in vitro and in vivo approaches to assess the ability of the lncRNA to suppress tumor growth. For the in vitro approach, we stably transfected the HCT-116 cell line, hypermethylated and silenced for TP53TG1, with a plasmid encoding the full-length lncRNA transcript. The efficiency of transfection was assessed by measuring TP53TG1 expression by quantitative RT-PCR (Fig. 2*A*). Upon TP53TG1 transfection, the cells proved to be significantly less proliferative in the 3-(4,5-dimethylthiazol-2-yl)-2,5-diphenyltetrazolium bromide (MTT) assay (Fig. 2*B*) and had a significantly lower percentage colony formation density (Fig. 2*B*) than empty vector-transfected cells. The reduced growth of the TP53TG1-transfected HCT-116 cell line was associated with apoptosis induction, based on the assessment of the sub-G1 cell population, caspase 3/7 levels, and the annexin V assay (Fig. 2*C*). The restoration of TP53TG1 expression upon transfection in HCT-116 was also associated with a decreased invasion and migration potential of these cells, as measured by the Matrigel-based xCELLigence real-time assay (31) (Fig. 2*D*) and the wound-healing assay (Fig. 2*D*).

For the in vivo approach, we first used tumor-formation assays in nude mice. HCT-116 cells transfected with either the empty or the TP53TG1 vector were s.c. injected into nude mice. Tumors originating from TP53TG1-transfected HCT-116 cells had a significantly lower volume and weight than empty vector-transfected/derived tumors (Fig. 2*E*), in addition to a higher apoptosis rate (Fig. 2*E*). We also did an orthotopic growth study, implanting equal-sized tumor pieces from the s.c. model into the colon tract. We observed that orthotopic TP53TG1-transfected tumors were significantly smaller than the empty vector-transfected tumors (Fig. 2*F*). We also proceeded with the converse experiment in which we analyzed the effect of TP53TG1 depletion in nontransformed immortalized colonocytes (HCECs), which have an unmethylated CpG island and express the lncRNA transcript. Upon efficient small interference RNA (siRNA)-mediated down-regulation of TP53TG1 (Fig. 2*G*), we observed a significant enhancement of cell viability, as measured by the MTT assay, relative to control siRNA-transfected cells (Fig. 2*G*), and a reduced apoptosis rate (Fig. 2*G*). Overall, our findings suggest that TP53TG1 has a tumor-suppressor role.

TP53TG1 Contributes to p53 Response to DNA Damage. p53 is known to activate TP53TG1 expression upon the induction of double-strand breaks in DNA caused by ionizing irradiation (27, 28) or treatment with DNA-damaging agents (27). This prompted us to consider whether TP53TG1 hypermethylation-associated silencing in cancer cells affected the sensitivity of chemotherapy drugs that directly target DNA. Using the TP53TG1-unmethylated HCEC line, which carries a wild-type p53 gene, we observed that treatment with the DNA-damaging agents caused not only the expected induction of p53 but also enhanced TP53TG1 expression (Fig. 3*A*). The same effect was observed in two other TP53TG1-unmethylated and p53 wild-type gastrointestinal cell lines: SW48 (colon) and SNU-1 (stomach) (Fig. 3*B*). However, we did not find increased TP53TG1 expression when using DNA-damaging agents in the unmethylated, but p53 mutant, SW-620 colorectal cancer cell line (Fig. 3*B*). Instead, we found that the induction of TP53TG1 upon DNA damage was dependent on the presence of a functional p53: siRNA-mediated depletion of p53 in HCECs impaired the overexpression of TP53TG1 when the DNA-damaging drug was used (Fig. 3*C*). We then attempted to determine how p53 exerted its control over TP53TG1 transcription at the molecular level. The chromatin immunoprecipitation (ChIP) assay revealed that p53 binds to a previously identified enhancer sequence located in intron 2 of TP53TG1 (32, 33) (Fig. 3*D*). The association of p53 to the TP53TG1 locus has been previously reported using ChIP followed by deep sequencing (ChIP-seq) (34). The described enhancer intronic region interacts with the promoter of TP53TG1, as shown by chromatin interaction analysis by paired-end tag sequencing (ChIA-PET) (35) (*SI Appendix*, Fig. S3). p53 binds to this regulatory region of TP53TG1 and transcriptionally activates it when the DNA-damaging agent is used (Fig. 3*D*). We observed the same binding pattern for the classical p53-responding gene $p21^{WAF1}$ (*SI Appendix*, Fig. S4).

Having discovered that TP53TG1 restoration in an initially methylation-silenced cell induces apoptosis and that p53 activates TP53TG1 transcription upon DNA damage, we wondered whether

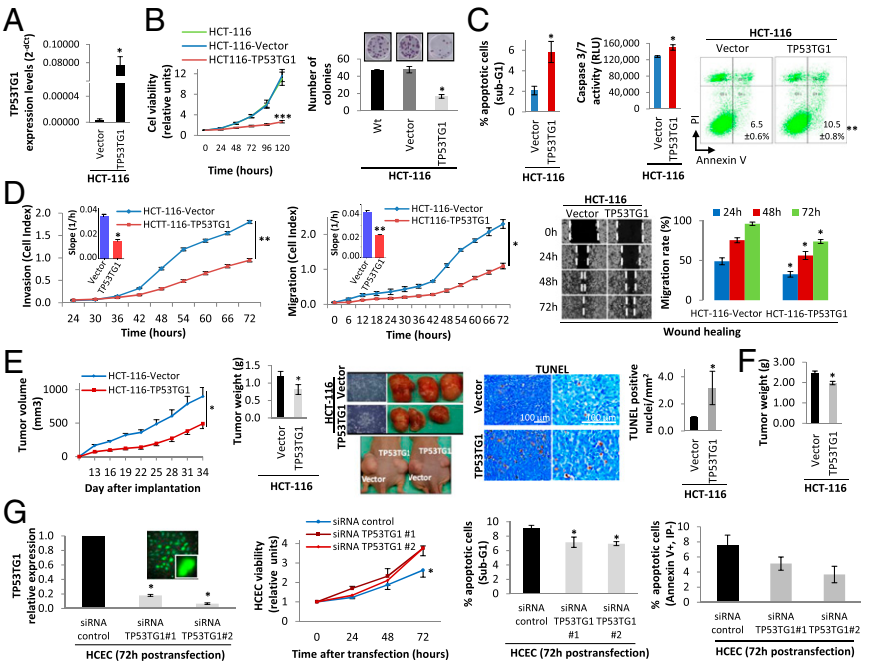

Fig. 2. TP53TG1 exhibits tumor-suppressor features in vitro and in vivo. (*A*) Efficient restoration of TP53TG1 upon transfection in HCT-116 cells according to qRT-PCR. Expression of TP53TG1 in cellular pools (four different clones) of HCT-116 stable transfected cells in comparison with the empty vector. Values were analyzed from triplicates and expressed as the mean ± SEM. (*B*) MTT and colony formation assays. TP53TG1 transfection reduces cell viability and the number of colonies in HCT-116 cells. (*C*) TP53TG1 restoration induces apoptosis in HCT-116 cells. Apoptotic cells were evaluated in TP53TG1 stably transfected HCT-116 cells after 24 h as the sub-G1 cell population and annexin V-positive/IP-negative cells by FACS analysis. Caspase 3/7 activity was determined after 24 h by a luminometric assay. Values are expressed as the mean ± SEM ($n = 6$). (*D*) TP53TG1 reduces invasion and migration properties in HCT-116 cells evaluated by the xCELLigence Real-Time (cell index) approach (*Left* and *Middle*) and the wound-healing assays ($n = 3$) (*Right*), respectively. (*E*) Growth inhibitory effect of TP53TG1 restitution in HCT-116 mouse tumor xenografts. (*Left*) Tumor volume ($n = 8$) was monitored over time. (*Middle Left*) Tumors were excised and weighed at 34 d. (*Middle*) Representative images of the confluence of HCT-116 stable transfected cells maintained in vitro for 7 d after implantation in mice and the size of the tumors at the end of the analyses. (*Middle Right*) Detection and (*Right*) quantification of apoptotic cells (in brown) from s.c. tumors by TUNEL assay ($n = 5$). (Scale bar, 100 μm.) (*F*) Growth-inhibitory effect of TP53TG1 restitution in HCT-116 cells in a colorectal orthotopic mouse model. Small pieces of the s.c. tumor model were implanted in the colon of nude mice, and tumor weight was measured after 30 d ($n = 4$–5). (*G*) Effect of TP53TG1 RNAi-mediated knockdown in the nontumorigenic HCEC line. (*Left*) Values were obtained by qRT-PCR and expressed as the mean ± SEM ($n = 3$). The photograph shows the transfection control efficiency (green). TP53TG1 down-regulation after 72 h reduces cell viability and apoptosis. Cell viability (*Middle Left*) was determined by MTT ($n = 3$) and the frequency of apoptotic cells was determined by FACS analysis of the sub-G1 cell population ($n = 3$) (*Middle Right*) and annexin V-positive/IP-negative cells (*Right*) ($n = 2$ for each independent siRNA). $^{**}P < 0.01$; $^{*}P < 0.05$.

the recovery of TP53TG1 expression sensitizes to DNA-damaging agents. To address this, we measured the IC_{50} of the HCT-116, TP53TG1-unmethylated, and p53 wild-type cell line, transfected with an empty vector or with the studied lncRNA for four different single-treatment DNA-damaging agents (doxorubicin, paclitaxel, carboplatin, and cisplatin) and the drug combinations used in the clinical context of colorectal cancer, 5-fluorouracil + oxaliplatin and 5-fluorouracil + irinotecan. We found that, in all of the cases, the transfection-mediated recovery of TP53TG1 expression significantly increased the sensitivity to these agents (Fig. 3*E*). We also extended the in vitro cell viability experiments to an in vivo mouse model of orthotopic growth. We observed that orthotopic colorectal tumors derived from TP53TG1-transfected HCT-116 cells were significantly more responsive to the common colorectal chemotherapeutic regimen of 5-fluorouracil + oxaliplatin than empty vector-derived tumors (Fig. 3*F*). These results indicate that TP53TG1 probably plays an important role in the p53-mediated antitumoral effects of DNA-damaging agents.

TP53TG1 Binds to the RNA Binding Protein YBX1 and Prevents Its Nuclear Localization. With the exception of its role as a transcript induced by p53 upon DNA damage (27, 28), nothing is known about the functions of TP53TG1. To identify protein partners of TP53TG1 that could characterize its activity in the processes described here, we performed RNA pull-down assays combined with mass spectrometry (MS). In vitro-synthesized full-length TP53TG1 RNA, or its antisense version, was incubated in the presence of HCEC extracts and the retrieved proteins were analyzed by SDS/PAGE. As shown in Fig. 4*A*, a protein band of ∼45 kDa was specifically pulled down by TP53TG1 RNA but not by other control RNAs. This band was cut out from the gel, trypsin-digested, and further characterized by MS, which identified the isolated band as the Y-box binding protein 1 (YBX1, also known as YB-1) through the identification of four distinct peptides (Fig. 4*B* and *SI Appendix*, Table S3). YBX1 functions as both a DNA and RNA binding protein and has been implicated in numerous cellular processes, including regulation of transcription and translation, pre-mRNA splicing, DNA reparation, and mRNA packaging (36). YBX1 activation has been associated with cancer progression (37, 38), the epithelial–mesenchymal transition (39), metastasis (40), and drug resistance (41, 42). Western blot with a specific antibody confirmed that YBX1 is enriched in the TP53TG1 pull-down (Fig. 4*C*). The reciprocal experiment showed that immunoprecipitation of YBX1 from HCECs can copurify the TP53TG1 lncRNA as a binding partner (Fig. 4*D*). Control IgG was used as a negative reaction and the YBX1 partner G3BP1 mRNA (43) was used as a positive control for YBX1 binding (Fig. 4*D*). Bioinformatic prediction of protein partners for TP53TG1 using the catRAPID system (44) also indicated that YBX1 was a likely target of the lncRNA studied here. We further characterized the specific RNA sequence in the TP53TG1 transcript that was responsible for the binding to the YBX1 protein. Using various YBX1 deletion mutants, followed by

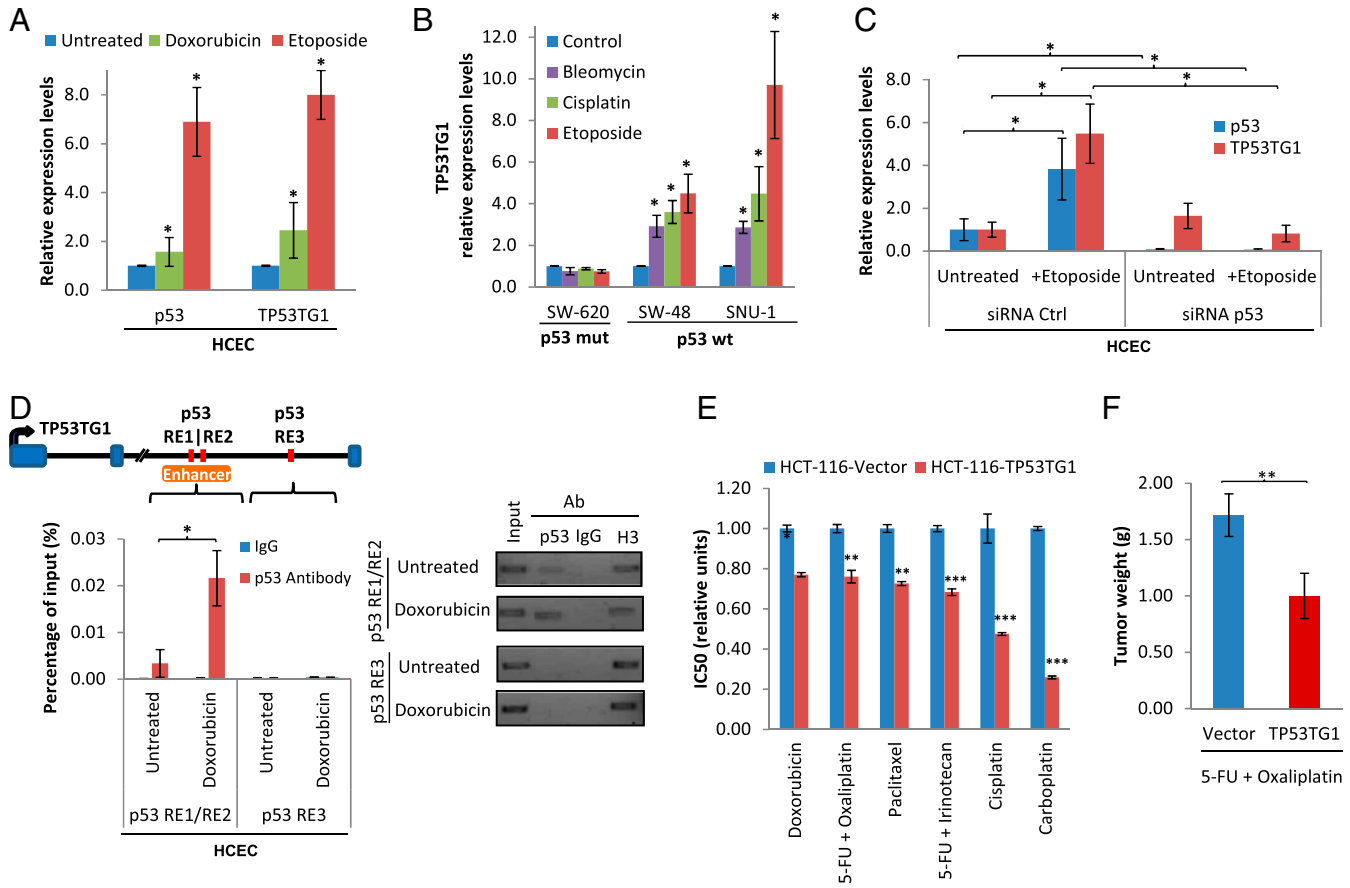

Fig. 3. DNA damage induces TP53TG1 expression in a p53-dependent manner. (*A*) Treatment with DNA-damaging agents increases p53 and TP53TG1 expression in TP53TG1-unmethylated and p53 wild-type HCECs. The cells were treated with doxorubicin (100 nM) or etoposide (50 μM) for 24 h. Values were obtained by qRT-PCR and expressed as the mean ± SEM ($n = 3$). (*B*) Treatment with DNA-damaging agents increases TP53TG1 expression in the TP53TG1-unmethylated and p53 wild-type colorectal (SW-48) and gastric (SNU-1) cancer cells but not in TP53TG1-unmethylated and p53 mutant colon cancer cells (SW-620). Cells were treated with bleomycin, cisplatin, and etoposide for 24 h. Expression was analyzed in triplicates by qRT-PCR, and the results are expressed as the mean ± SEM ($n = 4$). (*C*) TP53TG1 induction upon DNA damage depends on wild-type p53. p53 silencing by siRNA in HCECs prevents TP53TG1 activation upon 50 μM etoposide treatment for 24 h. Values were obtained by qRT-PCR and expressed as the mean ± SEM ($n = 3$). (*D*) The increase of TP53TG1 after DNA damage is mediated by direct binding of the p53 protein to p53 response elements (p53 REs) of the TP53TG1 gene. After doxorubicin (100 nM) treatment for 24 h in HCECs, ChiP was performed with IgG or p53 antibodies, followed by qPCR and semiquantitative PCR in the p53 RE region. Values of qPCR were obtained from triplicates and expressed as the mean ± SEM ($n = 3$). (*E*) Recovery of TP53TG1 expression restores chemosensitivity to DNA-damaging agents. TP53TG1 stably transfected HCT-116 cells were treated with various DNA-damaging anticancer drugs, and cell viability was determined by MTT. The half-maximal inhibitory concentration (IC_{50}) was calculated and expressed as relative units. (*F*) Orthotopic tumors derived from TP53TG1-transfected HCT-116 cells were more sensitive to 5-fluorouracil + oxaliplatin treatment than empty vector-derived tumors according to tumor weight. Significance of Mann-Whitney *U* test, ***$P < 0.001$; **$P < 0.01$; *$P < 0.05$.

YBX1 Western blot in the RNA pull-down assays, we identified that, from the 710 nucleotides of the full-length transcript, a middle region of 253 nucleotides was responsible for YBX1 binding (Fig. 4*E*). This region included five CACC YBX1 binding motifs (45, 46) (Fig. 4*E*). Most importantly, when we mutated the five CACC motifs, the binding of TP53TG1 to YBX1 was notably diminished (Fig. 4*E*). In addition, mobility shift assays showed that the recombinant YBX1 protein was able to bind specifically to this middle region, indicating a direct interaction with the lncRNA (Fig. 4*E*). The presence of the intact CACC YBX1-binding sites was necessary to ensure the tumor-suppressor function of TP53TG1 observed here, as transfection of the lncRNA form mutated at the five CACC motifs was unable to inhibit HCT-116 cell growth, as determined by the MTT and colony-formation assay (Fig. 4*F*). In addition, the cotransfection of the full-length wild-type YBX1 protein in TP53TG1-transfected HCT-116 cells increased their growth and invasion potential, thus reversing in part the tumor suppressor role of TP53TG1 (Fig. 4*G*). Our results therefore imply that the multitasked YBX1 protein is a direct target of TP53TG1 involved in its associated tumor suppressor features.

We then examined the effect that TP53TG1 could have on YBX1. The transfection-mediated restoration of TP53TG1 expression in HCT-116 did not affect the total mRNA or protein levels of YBX1 (Fig. 5*A*). In a similar manner, the siRNA-mediated depletion of TP53TG1 in HCECs affected neither the total transcript nor the amount of the YBX1 protein (Fig. 5*A*). There was also no association between the presence of TP53TG1 methylation-associated silencing in gastrointestinal cancer cell lines and YBX1 RNA levels (Fig. 5*A*). Thus, TP53TG1 does not seem to have a significant role in determining the overall levels of YBX1 in a particular cell or tumor. However, a key component of YBX1 activity resides in its controlled trafficking between the nucleus and the cytosol related to its dual activities as a DNA- and an RNA-binding protein (36, 41, 42). To assess the impact of TP53TG1 in YBX1 intracellular compartmentalization, we isolated and studied the nuclear and cytosolic fraction in our experimental system in detail. We found that YBX1 was present in the nuclear and cytosolic compartments of TP53TG1-methylated HCT-116 cells (Fig. 5*B*), but the transfection-mediated recovery of TP53TG1 expression in these cells caused the exclusion of YBX1 from the nucleus (Fig. 5*B*).

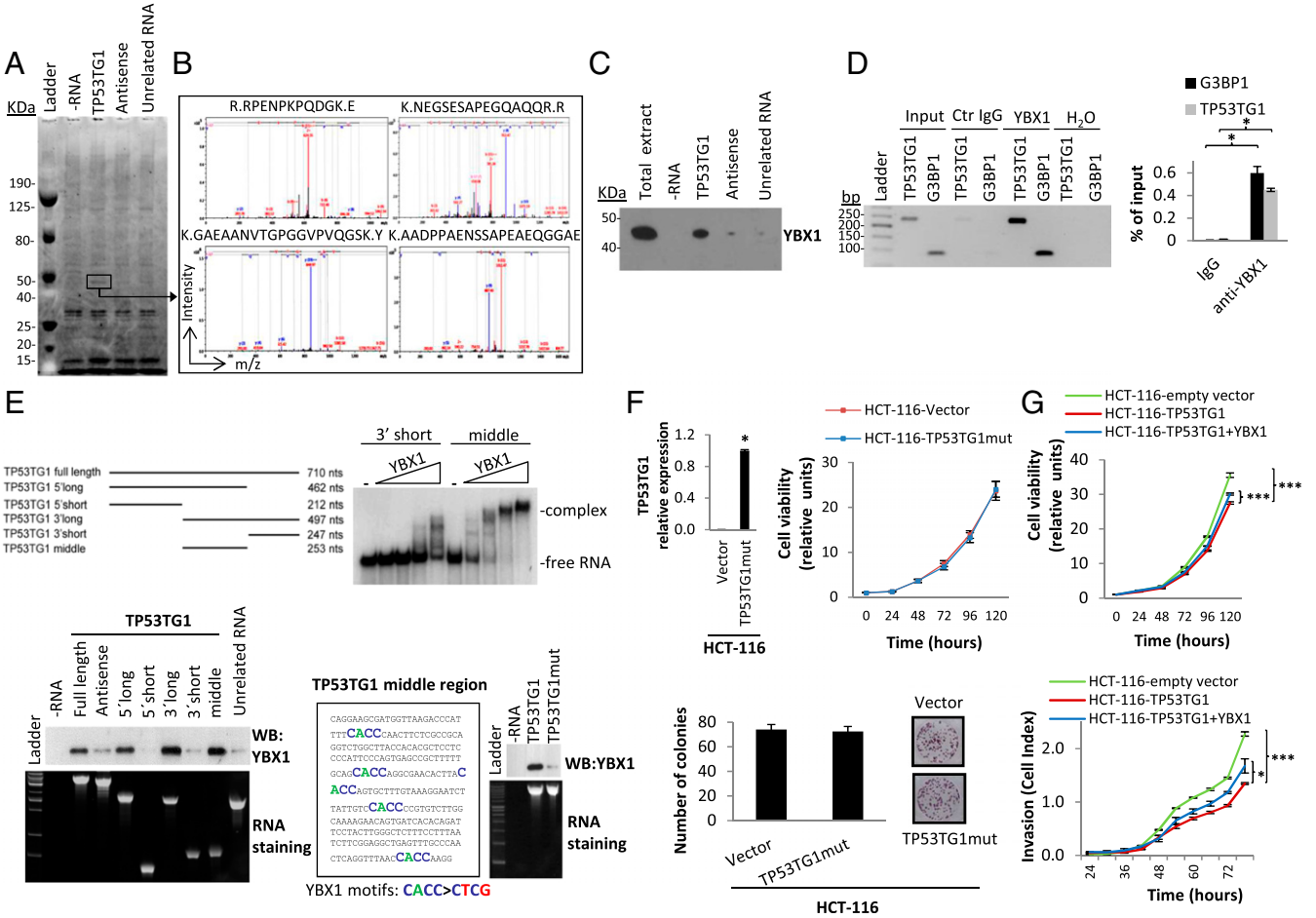

Fig. 4. TP53TG1 binds to the YBX1 protein. (*A*) Detection of candidate TP53TG1-associated proteins by RNA pull-down assays. In vitro-synthesized biotinylated full-length TP53TG1 lncRNA and other RNA control sequences were incubated in the presence of total HCEC extracts, retrieved with streptavidin beads, and the associated proteins were analyzed by SDS/PAGE. A specific band of ∼45 KDa (black square) was pulled down by TP53TG1 lncRNA. TP53TG1 antisense and unrelated RNA (Uc.160) were used as negative controls. (*B*) Identification of the TP53TG1 RNA isolated pull-down band by MS. The specific band detected in the RNA pull-down assay was cut out and trypsin-digested for MS analysis. The spectra show the four YBX1 peptides that bind to TP53TG1 lncRNA. (*C*) Western blot showing the specific association between YBX1 and TP53TG1 lncRNA in the samples obtained from the RNA pull-down. TP53TG1 antisense RNA and an unrelated RNA (Uc.160) were used as negative controls. Total extract of the TP53TG1 unmethylated HCEC line was used as the input control. (*D*) Confirmation of the YBX1 interaction with TP53TG1 by YBX1 immunoprecipitation (reverse pull-down). Endogenous YBX1 was immunoprecipitated from total HCEC extracts with anti-YBX1 antibody. The pulled-down RNA was extracted and analyzed by (*Left*) RT-PCR and (*Right*) qRT-PCR. The G3BP1 RNA was used as a positive target of YBX1. (*E*) YBX1 binds to the central region of TP53TG1. (*Upper* and *Lower Left*) Various truncated RNA fragments of TP53TG1 were pulled down following incubation with HCEC total extract, and YBX1 protein was detected by Western blot. TP53TG1 antisense and an unrelated RNA were used as negative controls. (*Upper Right*) Increasing amounts of recombinant YBX1 protein were incubated with either the 3′ end or the central region of the TP53TG1 transcript and run on a native 6% (wt/vol) acrylamide gel. The mobility shift indicates the direct interaction between YBX1 and TP53TG1. (*Lower Middle*) The middle sequence of TP53TG1 with the five YBX1 binding sites that were mutated is indicated. (*Lower Right*) RNA pull-down experiments show that mutation of these sites impairs the interaction. (*F*) Transfection of the TP53TG1 mutant form (*Upper Left*), unable to bind to the YBX1 protein, in HCT-116 cells does not affect growth determined by (*Upper Right*) MTT and (*Lower*) colony formation assays. (*G*) Cotransfection of the full-length wild-type YBX1 protein in TP53TG1-transfected HCT-116 cells increases (*Upper*) their growth (MTT) and (*Lower*) invasiveness (xCELLigence Real-Time). Values were expressed as the mean ± SEM ($n = 3$). ***$P < 0.001$; *$P < 0.05$.

Immunofluorescence assays confirmed the localization of YBX1 in the cytosol and nucleus of HCT-116 cells (Fig. 5*B*) and its exclusively cytosolic presence upon the transfection-related restoration of TP53TG1 expression (Fig. 5*B*). Using a panel of TP53TG1-methylated (KM12, TGBC11TKB, and KATO-III) and -unmethylated (HT-29, SW480, HCEC, GCIY, and NUG-3) gastrointestinal cells, we confirmed that nuclear staining was almost absent in the unmethylated cell lines and the clear detection of both nuclear and cytosolic localization in the hypermethylated samples (Fig. 5 *C* and *D*).

These results suggest that the tumor-suppressor role of TP53TG1 identified here could be mediated by preventing the widely described protumorigenic nuclear functions of YBX1 (36–42). YBX1 is known to bind to the promoter of the phosphatidylinositol-4,5-bisphosphate 3-kinase (PI3K) gene and to stimulate its transcription (47). Importantly for our observed chemoresistant phenotypes, it is known that PI3K stimulates AKT and MDM2 phosphorylation, thus facilitating p53 degradation (48). In our system, ChIP demonstrated that the transfection-mediated recovery of TP53TG1 expression in HCT-116 cells reduced the binding of the YBX1 protein to the PI3K promoter (Fig. 6*A*). Most importantly, the diminished binding of YBX1 to the PI3K promoter was associated with the down-regulation of the PI3K protein and the reduced phosphorylation of AKT in comparison with empty vector-transfected cells (Fig. 6*B*). Transfection of the TP53TG1 transcript mutated at the five CACC YBX1 binding sites did not affect PI3K protein levels or AKT phosphorylation (Fig. 6*B*). In addition, the

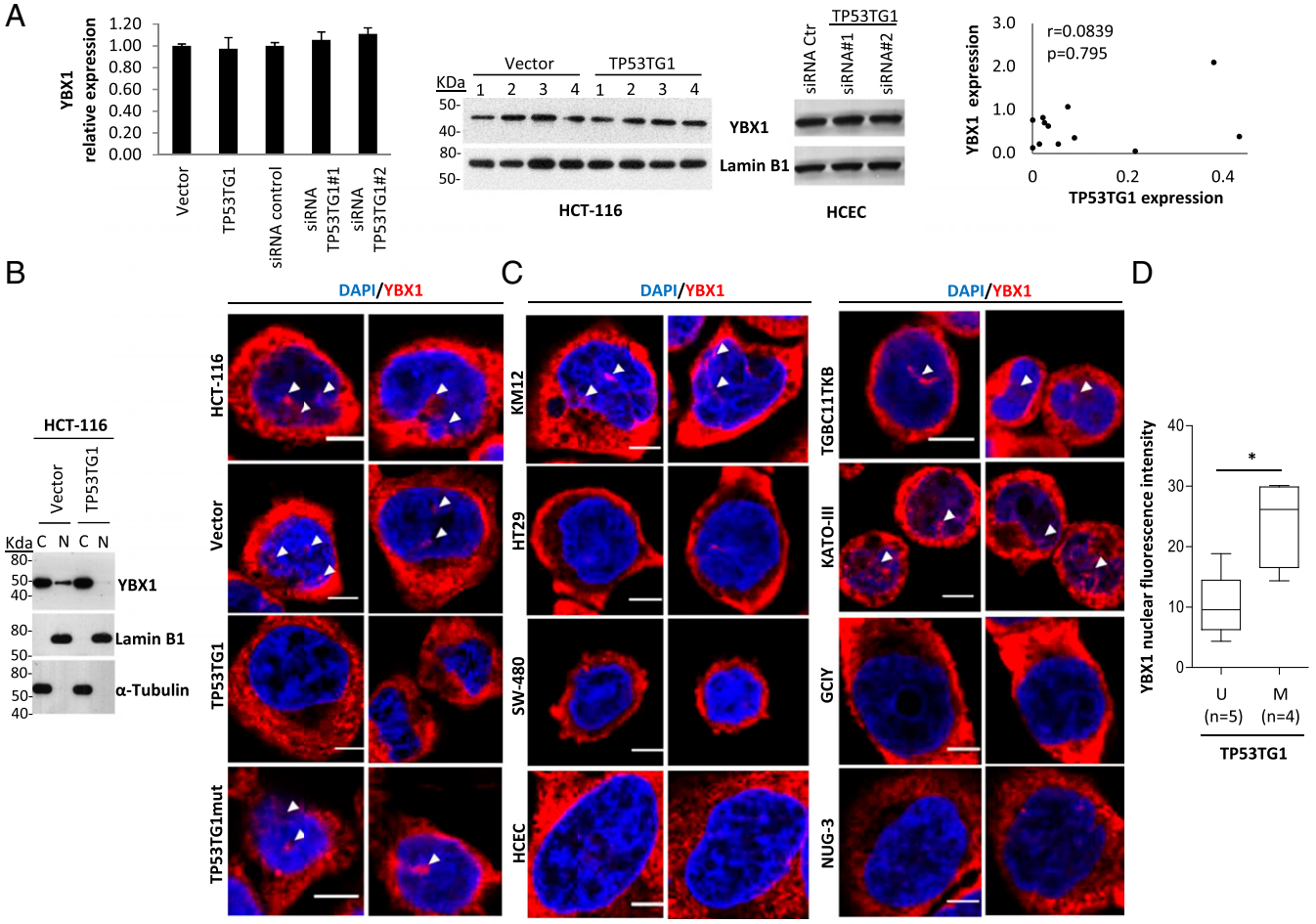

Fig. 5. TP53TG1 binds to the YBX1 protein, preventing its nuclear localization. (*A*) Lack of association between TP53TG1 and YBX1 expression levels. YBX1 expression levels were analyzed by qRT-PCR and Western blot after TP53TG1 stable overexpression in HCT-116 (four replicates: 1–4) and after TP53TG1 silencing by RNAi in HCECs. Expression levels of the TP53TG1 and YBX1 genes were determined by qRT-PCR in human colon and gastric cancer cell lines. Values of qRT-PCR were obtained from triplicates and expressed as the mean ± SEM (n = 3). (*B*) Recovery of TP53TG1 expression by transfection in the methylated HCT-116 cells modifies the subcellular distribution of the YBX1 protein. TP53TG1 restoration excludes the YBX1 protein from the nucleus according to subcellular fractionation experiments followed by Western blot (*Left*) and immunofluorescence assays (*Right*). (Scale bar, 5 μm.) White triangles indicate representative YBX1 expression in the nucleus. (*C*) Immunofluorescence assays confirm the nuclear exclusion of the YBX1 protein in the TP53TG1 unmethylated colorectal (HT-29, SW480, and HCEC) and gastric (GCIY and NUG-3) cell lines. Conversely, TP53TG1 hypermethylated and silenced colorectal (KM12) and gastric (TGBC11TKB and KATO-III) cell lines show nuclear localization, in addition to the cytosolic staining. (*D*) Quantification of nuclear immunofluorescence intensity (mean gray value) in the TP53TG1-unmethylated (HT-29, SW480, HCEC, GCIY, and NUG-3) and -methylated (HCT-116, KM12, TGBC11TKB, and KATO-III) cell lines. In the box plot, the central line represents the median and the limits show the upper and lower percentiles. Mann–Whitney *U* test, *P = 0.0317. M, methylated; U, methylated.

diminished PI3K/AKT signaling seen when TP53TG1 expression was restored was associated with greater sensitivity to PI3K and AKT inhibitors (Fig. 6*C*). Most importantly, the inhibition of the PI3K/AKT pathway upon TP53TG1 restitution also decreased MDM2 phosphorylation and estabilized p53 protein levels (Fig. 6*D*). These results therefore suggest that the epigenetic silencing of TP53TG1 in cancer cells promotes the YBX1-mediated activation of the PI3K/AKT pathway, which then creates further resistance not only to common chemotherapy DNA-damaging agents but also to small drug-targeted inhibitors. This finding relates to the broad spectrum of chemoresistance that is customarily associated with the YBX1 protein (36, 41, 42).

TP53TG1 Hypermethylation Occurs in Gastrointestinal Tumors in Association with Poor Outcome. The presence of TP53TG1 cancer-specific promoter CpG island hypermethylation was not an in vitro characteristic restricted to colorectal and gastric cancer cell lines. Data mining of large collections of primary human tumors interrogated by the same DNA methylation microarray platform as used here (26) confirmed the existence of TP53TG1 hypermethylation in 6% (12 of 180) and 10% (9 of 94) of colorectal (49) and gastric (50) tumors, respectively (Fig. 7*A*). The DNA methylation data available from The Cancer Genome Atlas (TCGA) for colorectal (51) and gastric (52) primary tumors also show the presence of TP53TG1 hypermethylation in 4% (14 of 369) and 13% (38 of 298) of these cases, respectively (Fig. 7*A*). The higher frequency of aberrant TP53TG1 DNA methylation noted in the primary stomach neoplasias prompted us to focus our efforts on this tumor type. TCGA RNA-sequencing data in gastric carcinomas (52) show that TP53TG1 methylation was associated with transcript down-regulation (Mann–Whitney *U* test, $P < 0.0001$) (Fig. 7*B*). Thus, we determined by methylation-specific PCR (MSP) the DNA methylation status of the 5′-end promoter CpG island of TP53TG1 in a collection of 173 primary gastric tumors. We found TP53TG1 hypermethylation in 26% (45 of 173) of the gastric neoplasms studied. We studied in greater depth the possible clinical impact of the epigenetic alteration in TP53TG1 in the 63 gastric cancer patients for whom we had detailed information about pathological characteristics and disease outcome. We found that the presence of TP53TG1 hypermethylation was significantly associated with shorter progression-free survival

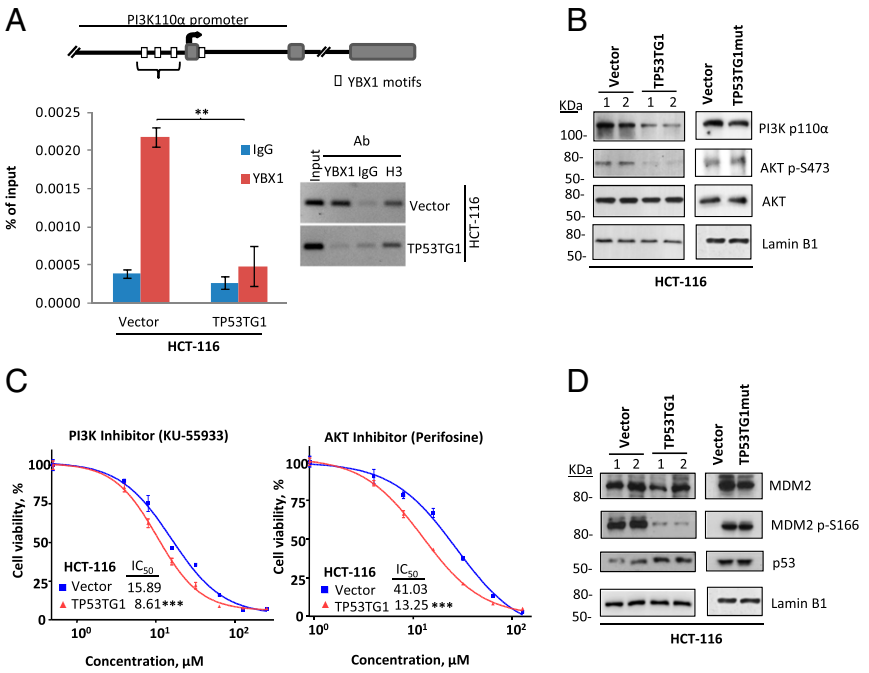

Fig. 6. TP53TG1 re-expression damps the YBX1-activated PI3K/AKT pathway and promotes sensitivity to targeted small drugs. (*A*) ChIP for the YBX1 protein in the PI3K promoter region. Restoration of TP53TG1 expression in HCT-116 cells inhibits the binding of the YBX1 protein to the PI3K regulatory region. (*B*) Western blot showing (*Left*) reduced expression of PI3K and lower phosphorylation levels of its downstream target AKT upon restitution of TP53TG1 expression in HCT-116 cells. (*Right*) Transfection of the TP53TG1 mutant form does not change PI3K expression or AKT phosphorylation levels. (*C*) Recovery of TP53TG1 expression enhances the sensitivity to (*Left*) PI3K and (*Right*) AKT small drug inhibitors. TP53TG1 or empty vector-transfected HCT-116 cells were treated for 48 h with KU-55933 (PI3K inhibitor) or perifosine (AKT inhibitor). Cell viability was measured by the MTT assay. Values of the half-maximal inhibitory concentration (IC_{50}) are shown. (*D*) Western blot showing (*Left*) reduced phosphorylation of MDM2 and stabilization of its target p53 upon expression of TP53TG1 in HCT-116 cells. (*Right*) Transfection of the TP53TG1 mutant form does not induce these changes. ***$P < 0.001$; **$P < 0.01$.

(PFS) ($P = 0.018$) (Fig. 7*C*). Considering the two groups of early and advanced clinical stage patients separately, we found that the impact of the outcome was due to the gastric patients with locoregional disease (stages I and II): TP53TG1 hypermethylation was significantly associated with shorter PFS in gastric patients with locoregional disease ($P = 0.028$) (Fig. 7*D*). Cox proportional hazard regression models of these conditions showed TP53TG1 methylation to be an independent prognostic factor of worse PFS [hazard ratio (HR) =3.64, 95% confidence interval (CI) =1.19–11.11, $P = 0.023$], compared with other parameters such as gender, age, histology, and tumor location (Fig. 7*E*). In addition, we assessed if the intracellular localization of YBX1, determined in part by TP53TG1 expression as we have shown in our in vitro experiments, could help to further discriminate the above described clinical groups. Using YBX1 immunohistochemistry, we observed that those patients with worse clinical outcome showed TP53TG1 hypermethylation and YBX1 nuclear staining, whereas the best PFS values were found in unmethylated TP53TG1 and cytosolic YBX1 cases ($P = 0.001$) (*SI Appendix*, Fig. S5). The impact of TP53TG1 methylation status in the clinical outcome of gastric cancer patients was also found in primary colorectal cancer tumors from the TCGA cohort (51). For these cases, TCGA RNA-sequencing data showed that TP53TG1 methylation was associated with transcript down-regulation (Mann–Whitney *U* test, $P < 0.0001$) (*SI Appendix*, Fig. S6), that TP53TG1 hypermethylation was significantly associated with shorter overall survival ($P = 0.03$) (*SI Appendix*, Fig. S6), and that TP53TG1 methylation was an independent prognostic factor of worse overall survival in Cox proportional hazard regression models (HR = 5.44, 95% CI = 1.15–25.68, $P = 0.032$) (*SI Appendix*, Fig. S6). Thus, TP53TG1 epigenetic disruption highlights those gastrointestinal malignancies that will be more clinically aggressive. These findings are consistent with the data obtained from the molecular, cellular, and mouse models.

Discussion

RNA expression patterns in human tumors that are distorted with respect to their normal tissue counterparts are one of the most commonly observed molecular phenotypes of carcinogenesis. Some of these RNA expression changes, due to genetic and/or epigenetic defects, are potential driver events of tumorigenesis, whereas others may be merely downstream bystander events that accompany cell transformation. Thus, in the expanding field of lncRNAs in cancer, it is important to distinguish events directly involved in the acquisition and development of the tumorigenic features from those that may be passengers in the process. One way to do this is to link the studied lncRNA with a well-defined oncogenic or tumor-suppressor pathway. In this paper, we have linked the promoter DNA methylation-associated silencing of the lncRNA TP53TG1 to the impaired response of the tumor-suppressor gene p53 to DNA damage that prevents the induction of apoptosis. Thus, the epigenetic inactivation of TP53TG1 can be considered to be another "hit" taken by the p53 network in cancer cells, in addition to the molecular disruption of other key elements of the p53 tumor suppressor and DNA damage response pathway, such as those occurring with the oncogene MDM2 and the tumor suppressor $p14^{ARF}$ (53, 54).

Another relevant step toward highlighting a functional role for a lncRNA in cancer cells, in addition to the in vitro and in vivo growth assays, is the characterization of a bona fide mechanism of action of the lncRNA with a probable role in tumorigenesis. One of the most difficult aspects in the field of lncRNA research is elucidating the exact cellular mechanism used by the molecule in question (12, 13). Combining RNA pull-down assays and MS, we have established that TP53TG1 binds and regulates the intracellular localization of the RNA binding protein YBX1, a factor that has attracted considerable interest among cancer researchers because it sits at the crossroads of several processes, such as tumor

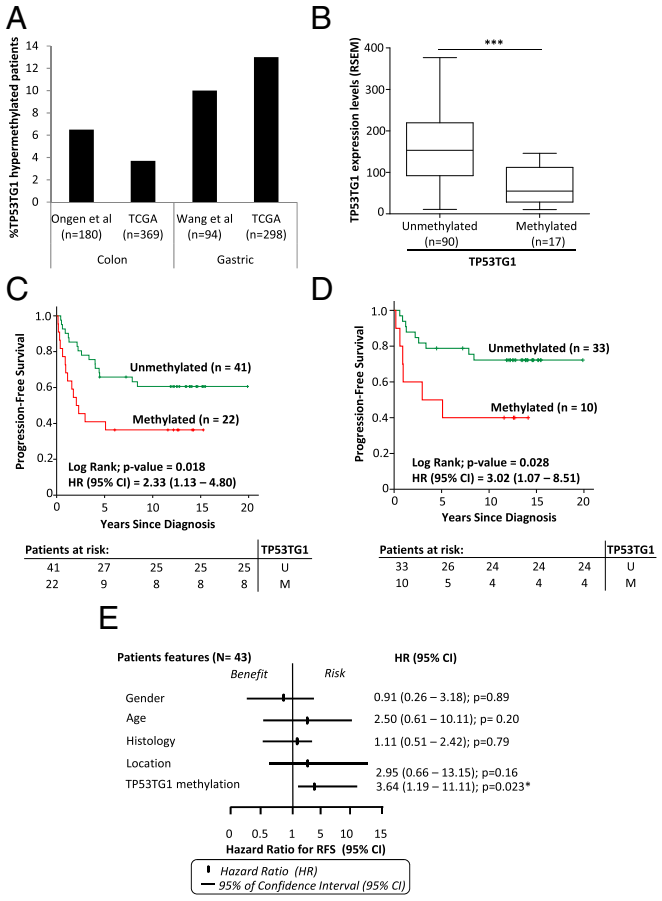

Fig. 7. Occurrence and impact of TP53TG1 hypermethylation in gastrointestinal cancer patients. (*A*) Frequency of TP53TG1 hypermethylation in primary colorectal and gastric tumors derived from TCGA and other publicly available datasets. (*B*) The presence of TP53TG1 methylation is significantly associated with loss of expression of the TP53TG1 transcript in primary gastric tumors from TCGA. The box plots illustrate the distribution of RNA-seq expression values; the central solid line indicates the median; the limits of the box show the upper and lower percentiles. Mann–Whitney *U* test, $***P < 0.0001$. (*C*) Kaplan–Meier curves showing that the presence of TP53TG1 hypermethylation in gastric cancer patients ($n = 63$) is significantly associated with shorter PFS ($P = 0.018$). CI, confidence interval; HR, hazard ratio; M, methylated TP53TG1; U, unmethylated TP53TG1. (*D*) TP53TG1 hypermethylation is an independent prognostic factor of shorter PFS in gastric patients with locoregional disease (stages I and II). Kaplan–Meier curves show that the presence of TP53TG1 hypermethylation in this group ($n = 43$) is significantly associated with shorter PFS ($P = 0.028$). (*E*) Forest plot representation of the Cox proportional hazard regression models, showing that TP53TG1 methylation is an independent prognostic factor of worse PFS (HR = 3.64, 95% CI = 1.19–11.11, $P = 0.023$) than other parameters such as gender, age, histology, and location.

progression (37, 38), epithelial–mesenchymal transition (39), metastasis (40), and drug resistance (36, 41, 42). In this article, we have described how YBX1 nuclear enrichment, mediated by TP53TG1 epigenetic loss, activates the growth-promoting PI3K gene and its downstream target, the oncoprotein AKT. Interestingly, the story goes back to the initial p53 link, because AKT activation induces MDM2 phosphorylation and final increased degradation of the tumor inhibitor p53. However, many other candidate genes and pathways could also be affected by the YBX1 aberrant nucleus–cytosol trafficking induced by the epigenetic loss of TP53TG1, and these alternative targets warrant further research in this area.

The cellular phenotypes arising upon TP53TG1 CpG island hypermethylation-associated silencing have implications beyond the observed molecular chain of events. They can have important translational consequences for the management of related neoplasms. A cancer cell featuring TP53TG1 epigenetic inactivation has acquired a chemoresistant phenotype affecting a wide repertoire of drugs. The DNA methylation-associated silencing of TP53TG1 is associated with resistance to compounds that damage DNA. These are commonly used classical chemotherapy drugs such as doxorubicin, irinotecan, carboplatin, cisplatin, and oxaliplatin, which are administered to treat the most prevalent human tumor types. Furthermore, the loss of TP53TG1 enhances the resistance to more specific next-generation small molecules such as PI3K and AKT inhibitors. The existence of this general chemoresistant phenotype partly explains why the oncology patients displaying the aberrant DNA methylation lesion in TP53TG1 have a shorter PFS. In this regard, the TP53TG1 hypermethylation described here would not only be an example of a tumor-suppressor lncRNA but could become a valuable marker in personalized cancer therapy if other studies were able to validate our findings in large, prospective, independent clinical trials.

Materials and Methods

Detailed materials and methods are provided in *SI Appendix, SI Materials and Methods*. The sequences of all primers and probes used in this study are listed in *SI Appendix*, Table S4.

All of the human colon cancer cell lines used in this study were purchased from the American Type Culture Collection (ATCC), except HCT-116 and DKO, which were generous gifts from Bert Vogelstein, Johns Hopkins Kimmel Comprehensive Cancer Center, Baltimore, MD. The immortalized nontumorigenic HCECs were kindly provided by Nestec Ltd. (29). The human gastric cancer cell lines MKN-45, MKN-7, TGBC11TKB, and GCIY were purchased from the RIKEN cell bank, KATO-III and SNU-1 were from the ATCC, and NUGC3 was from the Japanese Collection of Research Bioresources. DNA samples from surgically resected primary tumors were obtained from the Affiliated Hospital of School of Medicine (Tokyo Medical and Dental University) and from the University Hospital of Bellvitge–IDIBELL. All patients provided informed consent, and the study was conducted with the approval of the Institutional Review Board of the Bellvitge Biomedical Research Institute. Genome-wide DNA methylation analysis was performed with Illumina's 450K DNA methylation microarray (Infinium HumanMethylation450 BeadChip) as previously described (26). Using data from GENECODE v13 and the lncRNAdb database (55), we identified 280 lncRNAs included in the 450K array. DNA methylation analyses of candidate sequences were further validated by Bisulfite Genomic Sequencing and MSP. RACE was carried out with a SMARTer RACE cDNA Amplification Kit (Clontech). The noncoding nature of TP53TG1 was analyzed by the PhyloCSF comparative genomics method that yields the CSF and Western blot. The translation capacity of TP53TG1 was also evaluated in vitro with the TNT T7 Quick Coupled Transcription/Translation System (Promega). RNA expression was determined by semiquantitative and quantitative RT-PCR (qRT-PCR). Nuclear and cytoplasmic fractions were separated from 1 to 3×10^6 fresh cultured cells before total RNA and protein isolation (PARIS Kit, Ambion). Single-molecule RNA-FISH was performed using a pool of 28 probes tiling the TP53TG1 RNA coupled to Quasar 570 reporter dye. For stable TP53TG1 overexpression, the cDNA sequence of TP53TG1 (NR_015381; GRCh38/hg38) was cloned into the pcDNA4/T0 mammalian vector (Invitrogen), and cells were transfected with lipofectamine 2000 (Invitrogen). Silencing of TP53TG1 was performed with 50 nM of specific siRNA oligonucleotides (Qiagen) using lipofectamine 2000 (Invitrogen). Point mutations were introduced in the TP53TG1 sequence by site-directed mutagenesis using specific PCR primers and single-strand oligonucleotides. Cell viability and proliferation were determined by the MTT and colony formation assays. Induction of apoptosis was determined by the sub-G1 population percentage, annexin V staining, activity of caspase-3 and caspase-7, and in situ terminal transferase-mediated dUTP nick end labeling (TUNEL). The xCELLigence Real-Time assay was used to determine invasion and migration. Putative p53 transcription factor DNA-binding sites in the TP53TG1 gene were identified with the computer algorithm p53MH (56). ChIP was performed as previously described (22). In silico chromatin interaction was analyzed using publicly available ChIA-PET data (35). TP53TG1 protein interactors were identified by in-gel digestion and liquid chromatography–mass spectrometry/mass spectrometry (LC–MS/MS) analysis. The catRAPID omics algorithm (44) was used to estimate protein associations with the TP53TG1 lncRNA. RNA pull-down was performed essentially as described (57). Mouse xenograft and orthotopic experiments were performed as previously described (31). Statistical analyses were done using SPSS version 17.0 (SPSS) and GraphPad Prism version 5.04.

ACKNOWLEDGMENTS. We thank Diana Garcia, Carles Arribas, and Sebastian Moran [Genomics and Epigenomics Service, Cancer Epigenetics and Biology Program (PEBC), Bellvitge Biomedical Research Institute (IDIBELL)]; Nadia García [Unit of Nutrition and Cancer, Catalan Institute of Oncology (ICO), IDIBELL]; Carolina de la Torre and Silvia Barceló (Proteomics Service, IDIBELL); Esther Castaño [Centres Científics i Tecnològics de la Universitat de Barcelona (CCiTUB), Bellvitge, Universitat de Barcelona–IDIBELL]; and Carme Casal (Microscopy Service, PEBC, IDIBELL) for their technical support. This work was supported by the European Research Council under the European Community's Seventh Framework Programme (FP7/2007-2013)/ERC Grant Agreement 268626/EPINORC project; the Spanish Ministry of Economy and Competitiveness (MINECO Projects SAF2011-22803, PI13-01339, SAF2014-55000-R, and SAF2014-55000-R); the Instituto de Salud Carlos III (ISCIII), co-financed by the ERDF Fund "A Way to Achieve Europe," under the Integrated Project of Excellence PIE13/00022 (ONCOPROFILE); and Spanish Cancer Research Network (RTICC) Grant RD12/0036/0039, La Marató de TV3 Foundation Grant 20131610, the Cellex Foundation, and the Health and Science Departments of the Catalan Government (Generalitat de Catalunya) AGAUR Projects 2009SGR1315 and 2014SGR633. A.D.-L. is funded by Río Hortega Grant CM14/00067 from ISCIII. A.B.C. was funded by a research contract "Sara Borrell" (C09/00365) and CIBERobn from the ISCIII, Spain. J.S. is a Miguel Servet researcher at ISCIII. S.D. is funded by the German Research Foundation (DFG Di 1421/7-1) and the German Cancer Research Center (DKFZ). M.E. is an ICREA Research Professor.

1. Kapranov P, et al. (2007) RNA maps reveal new RNA classes and a possible function for pervasive transcription. *Science* 316(5830):1484–1488.
2. Esteller M (2011) Non-coding RNAs in human disease. *Nat Rev Genet* 12(12):861–874.
3. Djebali S, et al. (2012) Landscape of transcription in human cells. *Nature* 489(7414): 101–108.
4. Jonas S, Izaurralde E (2015) Towards a molecular understanding of microRNA-mediated gene silencing. *Nat Rev Genet* 16(7):421–433.
5. Adams BD, Kasinski AL, Slack FJ (2014) Aberrant regulation and function of microRNAs in cancer. *Curr Biol* 24(16):R762–R776.
6. Nana-Sinkam SP, Croce CM (2014) MicroRNA regulation of tumorigenesis, cancer progression and interpatient heterogeneity: Towards clinical use. *Genome Biol* 15(9): 445.
7. Rinn JL, Chang HY (2012) Genome regulation by long noncoding RNAs. *Annu Rev Biochem* 81:145–166.
8. Huarte M (2015) The emerging role of lncRNAs in cancer. *Nat Med* 21(11):1253–1261.
9. Liz J, Esteller M (2016) lncRNAs and microRNAs with a role in cancer development. *Biochim Biophys Acta* 1859(1):169–176.
10. Ling H, et al. (2015) Junk DNA and the long non-coding RNA twist in cancer genetics. *Oncogene* 34(39):5003–5011.
11. Kim J, et al. (2016) Long noncoding RNAs in diseases of aging. *Biochim Biophys Acta* 1859(1):209–221.
12. Bassett AR, et al. (2014) Considerations when investigating lncRNA function in vivo. *eLife* 3:e03058.
13. Guil S, Esteller M (2015) RNA-RNA interactions in gene regulation: The coding and noncoding players. *Trends Biochem Sci* 40(5):248–256.
14. Gupta RA, et al. (2010) Long non-coding RNA HOTAIR reprograms chromatin state to promote cancer metastasis. *Nature* 464(7291):1071–1076.
15. Gutschner T, et al. (2013) The noncoding RNA MALAT1 is a critical regulator of the metastasis phenotype of lung cancer cells. *Cancer Res* 73(3):1180–1189.
16. Huarte M, et al. (2010) A large intergenic noncoding RNA induced by p53 mediates global gene repression in the p53 response. *Cell* 142(3):409–419.
17. Liz J, et al. (2014) Regulation of pri-miRNA processing by a long noncoding RNA transcribed from an ultraconserved region. *Mol Cell* 55(1):138–147.
18. Feinberg AP (2007) Phenotypic plasticity and the epigenetics of human disease. *Nature* 447(7143):433–440.
19. Baylin SB, Jones PA (2011) A decade of exploring the cancer epigenome—Biological and translational implications. *Nat Rev Cancer* 11(10):726–734.
20. Weichenhan D, Plass C (2013) The evolving epigenome. *Hum Mol Genet* 22(R1):R1–R6.
21. Heyn H, Esteller M (2012) DNA methylation profiling in the clinic: Applications and challenges. *Nat Rev Genet* 13(10):679–692.
22. Lujambio A, et al. (2010) CpG island hypermethylation-associated silencing of non-coding RNAs transcribed from ultraconserved regions in human cancer. *Oncogene* 29(48):6390–6401.
23. Boque-Sastre R, et al. (2015) Head-to-head antisense transcription and R-loop formation promotes transcriptional activation. *Proc Natl Acad Sci USA* 112(18): 5785–5790.
24. Ferreira HJ, Heyn H, Moutinho C, Esteller M (2012) CpG island hypermethylation-associated silencing of small nucleolar RNAs in human cancer. *RNA Biol* 9(6):881–890.
25. Rhee I, et al. (2002) DNMT1 and DNMT3b cooperate to silence genes in human cancer cells. *Nature* 416(6880):552–556.
26. Sandoval J, et al. (2011) Validation of a DNA methylation microarray for 450,000 CpG sites in the human genome. *Epigenetics* 6(6):692–702.
27. Takei Y, Ishikawa S, Tokino T, Muto T, Nakamura Y (1998) Isolation of a novel TP53 target gene from a colon cancer cell line carrying a highly regulated wild-type TP53 expression system. *Genes Chromosomes Cancer* 23(1):1–9.
28. Kabacik S, Manning G, Raffy C, Bouffler S, Badie C (2015) Time, dose and ataxia telangiectasia mutated (ATM) status dependency of coding and noncoding RNA expression after ionizing radiation exposure. *Radiat Res* 183(3):325–337.
29. Poehlmann A, et al. (2013) Non-apoptotic function of caspases in a cellular model of hydrogen peroxide-associated colitis. *J Cell Mol Med* 17(7):901–913.
30. Lin MF, Jungreis I, Kellis M (2011) PhyloCSF: A comparative genomics method to distinguish protein coding and non-coding regions. *Bioinformatics* 27(13):i275–i282.
31. Vizoso M, et al. (2015) Epigenetic activation of a cryptic TBC1D16 transcript enhances melanoma progression by targeting EGFR. *Nat Med* 21(7):741–750.
32. Ernst J, et al. (2011) Mapping and analysis of chromatin state dynamics in nine human cell types. *Nature* 473(7345):43–49.
33. ENCODE Project Consortium (2012) An integrated encyclopedia of DNA elements in the human genome. *Nature* 489(7414):57–74.
34. Nikulenkov F, et al. (2012) Insights into p53 transcriptional function via genome-wide chromatin occupancy and gene expression analysis. *Cell Death Differ* 19(12): 1992–2002.
35. Li G, et al. (2012) Extensive promoter-centered chromatin interactions provide a topological basis for transcription regulation. *Cell* 148(1-2):84–98.
36. Kosnopfel C, Sinnberg T, Schittek B (2014) Y-box binding protein 1—A prognostic marker and target in tumour therapy. *Eur J Cell Biol* 93(1-2):61–70.
37. Jürchott K, et al. (2010) Identification of Y-box binding protein 1 as a core regulator of MEK/ERK pathway-dependent gene signatures in colorectal cancer cells. *PLoS Genet* 6(12):e1001231.
38. Goodarzi H, et al. (2015) Endogenous tRNA-derived fragments suppress breast cancer progression via YBX1 displacement. *Cell* 161(4):790–802.
39. Evdokimova V, et al. (2009) Translational activation of snail1 and other developmentally regulated transcription factors by YB-1 promotes an epithelial-mesenchymal transition. *Cancer Cell* 15(5):402–415.
40. El-Naggar AM, et al. (2015) Translational activation of HIF1α by YB-1 promotes sarcoma metastasis. *Cancer Cell* 27(5):682–697.
41. Bargou RC, et al. (1997) Nuclear localization and increased levels of transcription factor YB-1 in primary human breast cancers are associated with intrinsic MDR1 gene expression. *Nat Med* 3(4):447–450.
42. Dolfini D, Mantovani R (2013) Targeting the Y/CCAAT box in cancer: YB-1 (YBX1) or NF-Y? *Cell Death Differ* 20(5):676–685.
43. Somasekharan SP, et al. (2015) YB-1 regulates stress granule formation and tumor progression by translationally activating G3BP1. *J Cell Biol* 208(7):913–929.
44. Livi CM, Klus P, Delli Ponti R, Tartaglia GG (2016) catRAPID signature: Identification of ribonucleoproteins and RNA-binding regions. *Bioinformatics* 32(5):773–775.
45. Wei WJ, et al. (2012) YB-1 binds to CAUC motifs and stimulates exon inclusion by enhancing the recruitment of U2AF to weak polypyrimidine tracts. *Nucleic Acids Res* 40(17):8622–8636.
46. Ray D, et al. (2013) A compendium of RNA-binding motifs for decoding gene regulation. *Nature* 499(7457):172–177.
47. Astanehe A, et al. (2009) The transcriptional induction of PIK3CA in tumor cells is dependent on the oncoprotein Y-box binding protein-1. *Oncogene* 28(25):2406–2418.
48. Mayo LD, Dixon JE, Durden DL, Tonks NK, Donner DB (2002) PTEN protects p53 from Mdm2 and sensitizes cancer cells to chemotherapy. *J Biol Chem* 277(7):5484–5489.
49. Ongen H, et al. (2014) Putative cis-regulatory drivers in colorectal cancer. *Nature* 512(7512):87–90.
50. Wang K, et al. (2014) Whole-genome sequencing and comprehensive molecular profiling identify new driver mutations in gastric cancer. *Nat Genet* 46(6):573–582.
51. Cancer Genome Atlas Network (2012) Comprehensive molecular characterization of human colon and rectal cancer. *Nature* 487(7407):330–337.
52. Cancer Genome Atlas Research Network (2014) Comprehensive molecular characterization of gastric adenocarcinoma. *Nature* 513(7517):202–209.
53. Meek DW (2009) Tumour suppression by p53: A role for the DNA damage response? *Nat Rev Cancer* 9(10):714–723.
54. Li J, Kurokawa M (2015) Regulation of MDM2 stability after DNA damage. *J Cell Physiol* 230(10):2318–2327.
55. Amaral PP, Clark MB, Gascoigne DK, Dinger ME, Mattick JS (2011) lncRNAdb: A reference database for long noncoding RNAs. *Nucleic Acids Res* 39(Database issue): D146–D151.
56. Hoh J, et al. (2002) The p53MH algorithm and its application in detecting p53-responsive genes. *Proc Natl Acad Sci USA* 99(13):8467–8472.
57. Maamar H, Cabili MN, Rinn J, Raj A (2013) linc-HOXA1 is a noncoding RNA that represses Hoxa1 transcription in cis. *Genes Dev* 27(11):1260–1271.